

Fossil fuel resources, decarbonization, and economic growth drive the feasibility of Paris climate targets

Vivek Srikrishnan ^{*1}, Yawen Guan², Richard S. J. Tol^{3,4,5}, and Klaus Keller^{1,6}

¹Earth and Environmental Systems Institute, Pennsylvania State University, University Park, PA, USA

²Department of Statistics, North Carolina State University, Raleigh, NC, USA

³Department of Economics, University of Sussex, Sussex, United Kingdom

⁴Institute for Environmental Studies, Vrije Universiteit Amsterdam, Amsterdam, The Netherlands

⁵Department of Spatial Economics, Vrije Universiteit Amsterdam, Amsterdam, The Netherlands

⁶Department of Geosciences, Pennsylvania State University, University Park, PA, USA

*Corresponding author, vxs914@psu.edu

Abstract

Understanding how reducing carbon dioxide (CO_2) emissions impacts climate risks requires probabilistic projections of the baseline (“business-as-usual”) emissions. Previous studies deriving these baseline projections have broken important new ground, but are largely silent on two key questions: (i) What are the effects of deep uncertainties surrounding key assumptions such as remaining fossil fuel resources? (ii) Which uncertainties are the key drivers of the projected emissions and global warming? Here we calibrate a simple integrated assessment model using century-scale observations to project global emissions and committed temperature anomalies over the 21st century. We show that the projected emissions are highly sensitive to assumptions about available fossil fuel resources and decarbonization rates. We find that even under an optimistic, low-fossil fuel resources scenario, the median committed warming just by emitted CO_2 in 2100 exceeds the 1.5 degree Celsius Paris Agreement target. Across the analyzed scenarios, the probability of exceeding the 2 degree Celsius target just from emitted CO_2 ranges from 24% to 39%. The climate-system uncertainties and decarbonization rates are the key factors directly driving this uncertainty. Several economic growth parameters explain a large share of variability through their interactions.

1 Introduction

Anthropogenic carbon dioxide emissions drive climate risks. Emitted carbon can remain in the atmosphere for centuries to millennia [1]. Identifying the baseline risks associated with climate change requires projections under a “business-as-usual” (BAU), or no-policy, approach to continued emissions. There are several sources of uncertainty associated with these projections, including future population growth and the degree to which economic growth will require carbon emissions (via dependence on fossil fuel burning).

One approach to representing future emissions uncertainty is to derive scenarios which cover an appropriate range of not-improbable futures. Scenario generation avoids the assignment of probabilities to various outcomes. Such scenarios can be useful, for example, to inform exploratory modeling [2]. One downside of this approach is the lack of probabilistic information, which leaves scenario users guessing about the plausibility or likelihood of various futures [3]. The selection of which scenarios to quantify and communicate involves implicit, though hidden, probability assessments. Sound climate risk assessments requires probabilistic information [4, 5, 6, 7, 8, 9].

Another complication in developing projections of carbon emissions is that the fossil fuel resource base is deeply uncertain [10, 11, 12, 13, 14]. We use “resources” to refer to fossil fuel deposits which are potentially recoverable, as opposed to reserves, which are available for profitable extraction at current prices and technologies [15]. Additional uncertainty stems from uncertainties in fuel-specific emissions factors [16]. These uncertainties are important when evaluating the plausibility of various climate change narrative scenarios, such as SSP5 and RCP 8.5, which make specific assumptions about the future energy mix [17, 18].

Here we produce data-driven probabilistic assessments of global population, global economic output, and fossil fuel carbon dioxide (CO_2) emissions. The presence of deep uncertainties, such as varying fossil fuel resources or the penetration rate of zero-carbon technologies, complicates probabilistic analyses, as deep uncertainties cannot be assigned consensus

probability values. Here, probabilistic projections under deep uncertainties are understood as projections conditioned on a particular realization of those uncertainties. As a result, we investigate the influence of these deep uncertain factors on the resulting probability distributions through the use of scenarios. This approach allows us to understand how different realizations of deeply uncertain factors can be expected to influence future CO₂ emissions.

Previous studies differently navigate the trade-offs between two modeling objectives, realistic dynamics and sufficiently fast model evaluations for probabilistic calibration and tail resolution. On the one hand, models with a more detailed representation of economic and climate dynamics (*e.g.* [19, 20]) may not be able to be evaluated often enough to capture low-probability but high-risk tail areas of the predictive distribution, even with the use of sophisticated sampling techniques. On the other hand, statistical models (*e.g.* [21]), can be readily evaluated much more often, but may not be able to use mechanistic insights about system dynamics. Our approach uses a simple integrated assessment model, which allows us to these two competing modeling goals.

Building on the pioneering analysis in [22], our economic module uses a Solow-Swan growth model with a Cobb-Douglas production function. Economic growth is the result of growth in total factor productivity, labor inputs, and capital inputs, with the effect of labor and capital inputs determined by the elasticity of production (we assume that these elasticities add up to one, ensuring constant returns to scale). Emissions are determined through a mixture of four technologies: a zero-carbon pre-industrial technology, a high-carbon fossil fuel technology (representative of coal), a low-carbon intensity fossil fuel technology (representative of oil and natural gas), and a zero-carbon advanced technology (representative of renewables and nuclear). The rate of technology penetration, carbon intensities, and half-saturation years for the last three technologies are all treated as uncertain variables. We do not consider negative emissions technologies in this model due to critical uncertainties about the eventual range of technologies and required regulatory frameworks [23, 24, 25]. These unknowns make it difficult to construct prior distributions over important parameters, and due to a lack of data, these parameters are hard to meaningfully constrain.

For model calibration, we use a Bayesian data-assimilation framework (*e.g.* [26]) to combine prior information (including an expert assessment of per-capita economic growth [27]) with observational constraints. The Bayesian framework allows us to transparently generate probabilistic projections given a set of observations, structural assumptions, and clearly specified prior information. The observational constraints are based on century-scale data, from 1820-2014.

We use this modeling framework to address three main questions. First, what CO₂ emissions projections are consistent with this simple model and observational constraints? Second, how plausible are the Representative Concentration Pathways (RCPs) and other sets of scenario projections? Third, what are the key drivers and impacts of deep uncertainties on the probability of achieving temperature targets? We address this last question using scenario-based simulation and a global sensitivity analysis.

2 Methods

2.1 Data

We assimilate globally-aggregated observations from 1820-2014. Annual population and economic output data are from the 2018 Maddison Project dataset [28]. Economic output is the CGDPpc series, measuring real (i.e., inflation-corrected) income per capita with current international dollars (i.e., converting local currencies to US dollars based on their purchasing power) [28]. Annualized carbon emissions data from 1820-2014 [29] include emissions from fossil fuel burning, gas flaring, and cement manufacturing, and exclude emissions related to land-use changes.

2.2 Model Structure

We use a simple model structure, typical of top-down integrated assessment models [30, 31], to facilitate the uncertainty analysis. Outputs are globally-aggregated population (in billions), gross world product (in trillions 2011 US\$), and carbon emissions (in Gt C/yr), with an annual temporal resolution. The model generates these outputs using a set of three coupled modules: (1) population; (2) economic output; (3) carbon emissions.¹ There is a bidirectional coupling between population and economic output: population affects labor inputs through the labor force participation rate, while per-capita income affects the rate of population growth. CO₂ emissions are a consequence of by economic output through a mixture of emitting technologies with varying emissions intensities.

Population

We model population growth using a logistic model [32], modified by an income-sensitive growth rate. At time t , population P_t is given by

$$P_t = P_{t-1} \left[1 + \left(\psi_1 \frac{y_{t-1}}{\psi_2 + y_{t-1}} \right) \frac{\psi_3 - P_{t-1}}{\psi_3} \right], \quad (1)$$

where y is annual per-capita income, ψ_1 is the annual population growth rate, ψ_2 is the half-saturation parameters with respect to per-capita consumption, and ψ_3 is the logistic carrying capacity. This model structure allows for interactions between per-capita income and population growth. Note that Equation (1) implies that the population grows before stabilizing near saturation; other projections have been made which assume population peaks and then decreases [33].

Economic Output

To model gross world product, we use a Cobb-Douglas production function in a Solow-Swan model of economic growth. Total world production Q_t at time t is

$$Q_t = A_t L_t^\lambda K_t^{1-\lambda}, \quad (2)$$

¹We could have followed the Kaya Identity and include energy use. However, carbon dioxide emissions are not measured but instead imputed from energy use. Including energy use would not add information, but it would increase the dimensionality of the model.

where A is total factor productivity, L is labor input, K is capital input, and λ is the elasticity of production with respect to labor. Each year, total production is divided between consumption and investment,

$$Q_t = U_t + I_t = (1 - s)Q_t + sQ_t, \quad (3)$$

where s is the savings rate, which we assume to be constant.

Growth in total factor productivity (TFP) occurs exogenously. The dynamics of long-term technological change are deeply uncertain [34, 35]. Following [7], we allow for TFP to saturate as the population ages and become less innovative:

$$A_t = A_{t-1} + \alpha A_{t-1} \left[1 - \frac{A_{t-1}}{A_s} \right], \quad (4)$$

where α is the TFP growth rate and A_s is the TFP saturation level.

Capital stock growth occurs through a balance of depreciation and investment from the previous time step,

$$K_t = (1 - \delta)K_{t-1} + I_{t-1}, \quad (5)$$

where δ is the capital depreciation rate, which is constrained to be less than the savings rate s . Labor input is determined by

$$L_t = \pi P_t, \quad (6)$$

where π is the labor force participation rate. Labor is initialized using the (uncertain) initial population P_0 , while capital is initialized using the steady-state relationship

$$K_0 = \left(\frac{sA_0}{\delta} \right)^{1/\lambda} L_0. \quad (7)$$

Carbon Emissions

We model the link between economic output and anthropogenic CO₂ emissions from fossil fuel burning and cement production using a time-dependent carbon intensity of production. That is, we assume that energy is a derived demand, rather than a factor of production. The carbon emissions C_t at time t are

$$C_t = Q_t \phi_t, \quad (8)$$

where ϕ is the carbon intensity. ϕ is modeled as a weighted average of four broadly defined technologies,

$$\phi_t = \sum_{i=1}^4 \gamma_{i,t} \rho_i, \quad (9)$$

where $\gamma_{i,t}$ is the fraction of the economy invested in technology i , which has a technology-specific carbon intensity ρ_i . This assumes that each fuel is used uniformly across end-uses. We set the carbon intensity of technology 1 to zero to represent pre-industrial economic activity, which had negligible fossil fuel emissions (while human activity did produce CO₂ emissions during this period [36], the primary driver of these emissions was land-use change, which we do not consider). The carbon intensities of the technologies 2 and 3 are estimated

from observations with the constraint $\rho_2 \geq \rho_3$. This constraint represents the transition from a higher carbon intensity technology, analogous to coal, to a lower carbon intensity technology, analogous to oil and natural gas. We set the carbon intensity of technology 4 to zero to simulate the penetration of low-carbon technologies such as nuclear and renewables. The time dynamics of γ_i are approximated as logistic penetration curves,

$$\gamma_{1,t} = 1 - \frac{1}{1 + e^{-\kappa(t-\tau_2)}} \quad (10)$$

$$\gamma_{2,t} = \frac{1}{1 + e^{-\kappa(t-\tau_2)}} - \frac{1}{1 + e^{-\kappa(t-\tau_3)}} \quad (11)$$

$$\gamma_{3,t} = \frac{1}{1 + e^{-\kappa(t-\tau_3)}} - \frac{1}{1 + e^{-\kappa(t-\tau_4)}}, \quad \text{and} \quad (12)$$

$$\gamma_{4,t} = \frac{1}{1 + e^{-\kappa(t-\tau_4)}}, \quad (13)$$

where κ is the rate at which technologies penetrate and τ_i is the time at which technology i has penetrated half the market. This type of logistic penetration model can reasonably approximate observed energy substitution dynamics [37, 38].

To account for the non-renewable nature of fossil fuels, we impose a limit on the total emissions from 1700 to 2500. The base-case limit is set to 6,000 GtC, as in the DICE integrated assessment model [30]. To understand the impact of this deeply uncertainty limit, we also consider two alternate fossil fuel resource scenarios, based on the literature: a “low” scenario of 3,000 Gt C available from 2015 to 2500 [39] and a “high” scenario of 10,000 Gt C available over the same period [40]. The assumed resource base primarily affects parameter τ_4 .

2.3 Calibration

We use Bayesian data-assimilation to calibrate the model and estimate parametric and predictive uncertainty. Bayesian statistical methods allow for the fusion of data with prior information via Bayes’ theorem [41], yielding probabilistic parameter estimates and projections. Prior distributions represent a transparent method for incorporating exogenous information and structural assumptions into the calibrating process (see Table S1 for a table of prior distributions for the seventeen uncertain model parameters).

Bayes’ theorem requires the specification of the likelihood of the observations given the model parameters. Mis-specification of the model discrepancy structure, or the statistical distribution of model residuals, can result in biased estimates [42]. As our model outputs are necessarily greater than zero, we construct our likelihood function using log-scale residuals.

The simplest choice is to represent the model residuals as independent and identically distributed (i.i.d.) Gaussian noise. To investigate the validity of this assumption, we use a differential evolution algorithm [43, 44] to find a maximum *a posteriori* (MAP) estimate. The model fits and residuals corresponding to this estimate are shown in Fig. S3. Contrary to the i.i.d. assumption, the residuals are auto- and cross-correlated. As a result, we use a vector autoregressive representation for model discrepancy. We also allow for i.i.d. observation errors in each data series. The mathematical specification of the combined error structure

model and derivation of the corresponding likelihood function is provided in the Supplemental Material. Prior distributions for the fifteen statistical parameters are shown in Table S2.

We use Markov Chain Monte Carlo (MCMC) with the Metropolis-Hastings algorithm [45, 46] to draw samples from the posterior distribution for each modeling scenario. Four chains are run to facilitate convergence checks. Each chain is initialized at a MAP estimate for that scenario and is run for two million iterations. A burn-in period of 500,000 iterations is discarded at the start of each chain. Both the chain and burn-in lengths are determined using a combination of visual inspection and the Gelman-Rubin diagnostic [47]. Plots of the resulting marginal posterior distributions and the pairs plot are provided in Figs. SI2 and SI3.

3 Results

3.1 Hindcast Skill and CO₂ Projections

Our model, while relatively simple, captures historical dynamics reasonably well. We assess the hindcast skill through a cross-validation experiment. We randomly sample fifty hold-out sets (consisting of thirty-nine years, or one-fifth the data series length). The model is calibrated with the remaining data, and simulations for the held-out data are generated, conditional on the calibration data. We look at the deviation of predicted to actual data coverage for the 90% credible interval. This difference reflects the reliability of the probabilistic output [48], as a projection which is neither over- nor under-confident will cover the data at the appropriate fraction. The average coverage of the 90% credible interval on the held-out data is 93% for population and economic output and 92% for emissions.

Using the posterior distribution from the calibration procedure, we simulate 100,000 future trajectories of population, economic output, and CO₂ emissions, conditional on the observed data. The 90% credible interval at each year, along with the marginal emissions in 2100, are shown in Fig. 1 (the “base” scenario). Our model’s marginal yearly emissions distribution in 2100 has a shorter upper tail than in [21]. This may be partially due to the different data window used in their model calibration (1960-2010). When we calibrate our model with data from 1950-2014, the resulting projections (Fig. S5) of population are more confident than our baseline projections (possibly from missing fluctuations such as those due to the World War 2), there is an upward increase in projected economic growth (likely from only assimilating the post-World War 2 boom), and emissions projections are less confident.

The extended lower portion of our projections (both baseline and based on 1950-2014 data) are missing from the projections in [21] due to differences in model structure, as we allow for substitution of a zero-carbon technology for fossil fuel-emitting technologies, as opposed to their random-walk-with-trend approach to decreasing emissions intensity. Indeed, median projected emissions peak in the 2050s and 2060s at around 12 Gt C/year, with a slight reduction to 11 Gt C/yr in 2100. This median estimate in 2100 is lower than the median estimate from [21]. Many of the posterior samples corresponding to lower emissions involve global zero-carbon half-saturation in the first half of the 21st century, which would require unprecedented improvements in global energy intensity [50]. We do not *a priori* rule out more rapid decarbonization. Weaker prior belief that the global half-saturation of zero-

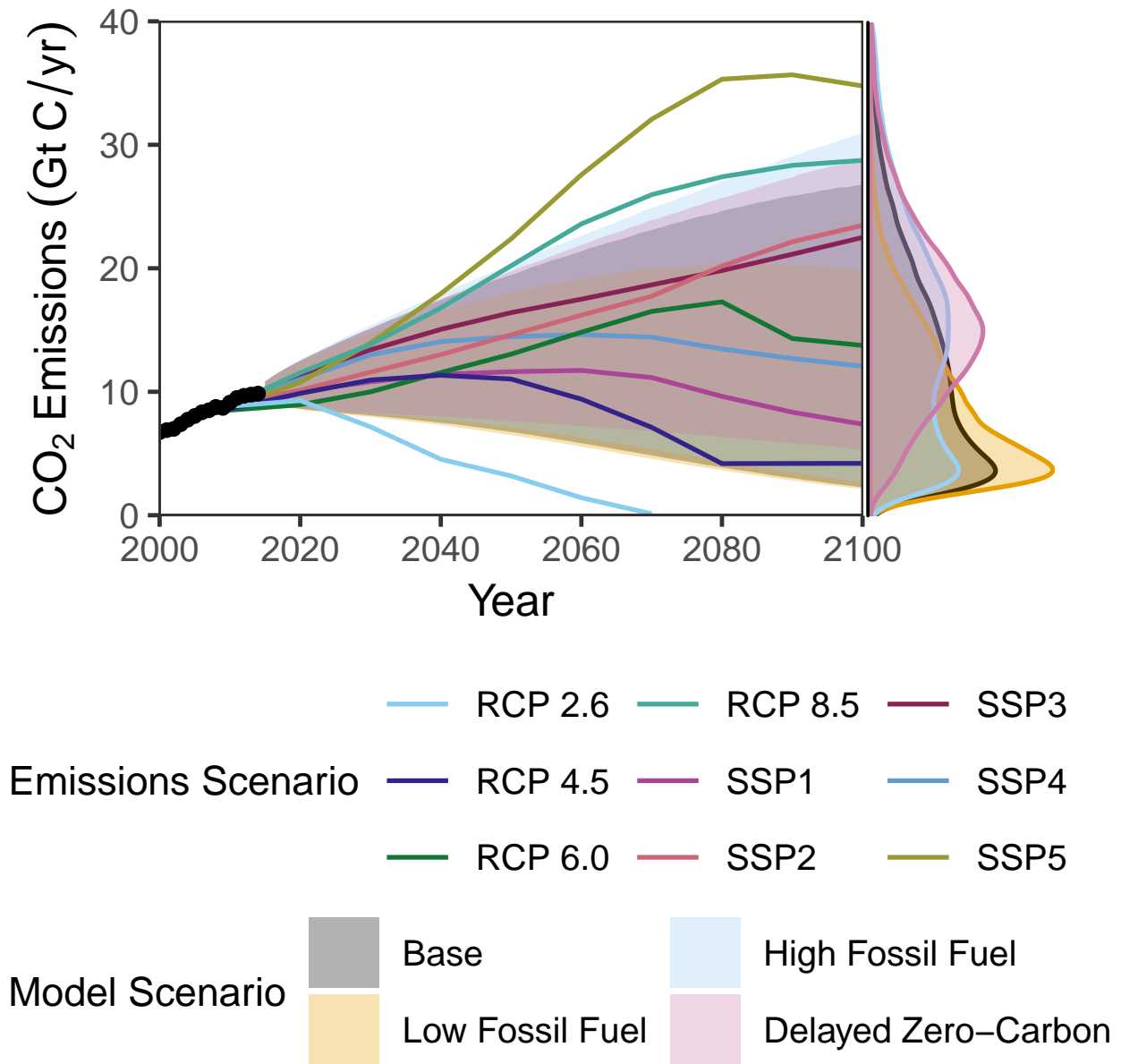


Figure 1: **Projections of carbon dioxide emissions** – Projections are for four model scenarios: a) the base scenario; b) the low fossil fuel scenario; c) the high fossil fuel scenario; and d) the delayed zero-carbon scenario. The shaded regions are the 90% credible intervals. Black dots are observations. The marginal distribution of projected business-as-usual CO₂ emissions in 2100 is shown on the right. Marker baseline Shared Socioeconomic Pathways (SSPs) [18] and Representative Concentration Pathways (RCPs) [49] CO₂ emission trajectories are shown for comparison.

carbon technology will occur in the 21st century would result in this lower mode shrinking or disappearing. An example of this is the “zero-carbon” scenario from Fig. 1, which places 2.5% prior probability on these rates of decarbonization.

3.2 How Plausible Are Future Emissions Scenarios?

One important question is how representative and plausible the Representative Concentration Pathways (RCPs) [51] and Shared Socioeconomic Pathways (SSPs) [52, 53] are as scenarios for future climate impacts under the BAU assumption. It is important to note that unlike the RCPs, the SSPs combine emissions scenarios with a series of assumptions related to socioeconomic development [18]. These additional assumptions influence the potential consequences of climate change by representing differences in the ability of the world to adapt to changing climate risks [52]. Fig. 1 (base scenario) shows how the CO₂ emissions associated with the RCPs and SSPs align with our projections throughout the rest of the 21st century. Tab. 1 summarizes the percentiles associated with each emissions scenario based on projected emissions in 2100.

Table 1: **Percentiles of CO₂ emissions scenarios in 2100 by model scenario** – Percentiles of CO₂ emissions in 2100 for each marker RCP and SSP scenario by model scenario. RCP 2.6 is omitted as we exclude negative-emissions technologies.

Model Scenario	Base	Low Fossil Fuel	High Fossil Fuel	Delayed Zero-Carbon
RCP 4.5	18%	25%	12%	3%
RCP 6.0	64%	80%	48%	39%
RCP 8.5	97%	>99%	93%	95%
SSP1	36%	50%	25%	10%
SSP2	91%	98%	84%	86%
SSP3	89%	98%	82%	83%
SSP4	57%	73%	42%	30%
SSP5	99%	>99%	98%	99%

Our projections cannot capture the dynamics associated with RCP 2.6 as our model does not consider negative-emissions technologies. While RCP 4.5 appears to be an outlier relative to the SSP narrative scenarios, it is representative of the lower mode of the distribution, which includes states of the world in which the penetration of zero-carbon technologies is rapid, which can include up to 25% of the probability mass in our low-fossil fuel scenario. When zero-carbon penetration is delayed, the lower mode disappears (see Fig. 1 and Tab. 1). RCP 6.0 is more representative of the central mode of the distribution, which includes states of the world with slower decarbonization as well as slower levels of economic growth, though the dual deep uncertainties of fossil fuel resource availability and decarbonization rates strongly affect the relative probability of this scenario.

The underlying socioeconomic development assumptions for RCP 8.5 involve considerably increased burning of coal [17] (represented in our model as technology 2). Our model suggests that RCP 8.5 is characteristic of the upper tail (beyond the 90% percentile, as in Tab. 1) of 21st century BAU emissions for most of the century, which agrees with the analysis in [21].

Simulations in this upper tail, with emissions in 2100 greater than 30 Gt C/yr, are largely characterized by a combination of three factors: (i) faster economic growth due to a reduced depreciation rate of capital stock; (ii) higher median emissions associated with technology 3 (the lower-emitting of the two non-zero emissions technologies, analogous to natural gas); and (iii) slower penetration of zero-carbon technologies. As such, while RCP 8.5 is not a best estimate of a BAU emissions trajectory, it can serve a valuable purpose as an example of a high-risk (if relatively low-probability) scenario. This is particularly acute as the forcings associated with RCP 8.5 could be achieved with lower emissions than those associated with the scenario due to uncertainties in the Earth’s carbon cycle [54].

Most of the quantitative scenarios associated with SSPs 1-4 span the central 90% credible interval of emissions in our base scenario, suggesting that these scenarios may capture the very likely (as used by IPCC AR5 [55]) range of 21st century CO₂ emissions. The CO₂ emissions associated with SSP5 are far into the tail of our model’s projections, in the 98% or 99% percentile. This is, perhaps, not surprising given the “return to coal” assumption in that scenario [56, 57].

One of the key assumptions in calibrating this model is the upper constraint on emissions from fossil fuels. The amount of fossil fuel resources are deeply uncertain [11, 12, 14]. To explore the effect of this deep uncertainty, we examine two additional scenarios: a “low-fossil fuel” scenario, in which 3,000 Gt C are available from 2015 on, and a “high-fossil fuel” scenario, in which 10,000 Gt C are available. The low-fossil fuel scenario is based off the resource estimates in [39], while the high-fossil fuel scenario is based off the resource estimates in IPCC AR5 [40]. In both cases, we use the total resource size estimate, rather than disaggregating or limiting only to the oil/gas resource base. If only those resources are considered (due to the way in which technologies are mixed in the emissions model), the corresponding estimates would be lower, though, the effect of this reduction in the available resource base should be in line with the trends from our scenario analysis. The fossil fuel constraint primarily influences the marginal posterior distribution of τ_4 (Fig. S6), and therefore the rate at which economic growth and emissions are decoupled. The 90% central credible intervals for the other marginal posteriors are the same regardless of the fossil fuel scenario.

As, perhaps, expected, under the BAU assumption, zero-carbon penetration is allowed to be delayed as more fossil fuel resources are available. The resulting impacts on projected emissions are shown in Fig. 1 and Tab. 1. Under the low fossil-fuel scenario, the projected marginal distribution in 2100 becomes unimodal (albeit with a long tail), as simulations with rapid economic growth require prompt decarbonization to avoid running out of fossil fuel resources. RCP 4.5 captures the emissions trajectories associated with these scenarios, while RCP 6.0 is representative of future states of the world with slower economic growth, and hence less pressure to decarbonize. The only SSPs included within the 90% credible interval are SSPs 1 and 4, with no probability mass associated with the emissions trajectories associated with RCP 8.5 and SSP5. This agrees with analyses which have criticized these two scenarios on the basis of energy resource availability [14, 57]. Even if coal resources are widespread, without a global “return to coal,” the important remaining resources are oil and gas deposits, which are smaller in terms of expected emissions [39] and deeply uncertain, particularly with respect to unconventional resources [11, 12].

On the other hand, when more fossil fuel resources are available (as in the high-fossil

fuel scenario), more rapid economic growth can occur while decarbonization is postponed. This results in a larger upper mode (greater emissions) and a longer tail, so that RCP 6.0 is almost the median scenario and RCP 8.5 is contained within the central 90% credible interval.

3.3 What Are the Key Drivers of Temperature Anomaly Projections?

Our interest in projecting CO₂ emissions is to estimate the impact of projected 21st century cumulative CO₂ emissions on global mean temperature anomalies. On very short time scales, changes in global mean temperatures are proportional to cumulative emissions [58]. The proportionality constant is the *Transient Climate Response to cumulative carbon Emissions* (TCRE) [59]. This linear relationship may not be the same for all levels of atmospheric carbon, but there is evidence that it is a good approximation below cumulative emissions of 2000 Gt C [60].

Our temperature anomaly calculations are based on the HadCRUT4 dataset [61]. We compute anomalies using cumulative emissions from 1870, relative to the average 1860–1881 global mean temperature, for symmetry with IPCC AR5 [62]. Uncertainty in the TCRE is captured using a log-normal distribution fit to the 5-95% range from [59]. The resulting anomalies (Figure 2), which are the anomalies committed to (not immediately observed) by cumulative emissions, are likely underestimates of the eventually observed anomalies. This is due to our focus only on CO₂ emissions, neglecting other greenhouse gases, which reduce the carbon budgets required to achieve particular temperature targets [63]. These other greenhouse gases have varying reduction potentials depending on gas and sector [64].

The median and 95% percentile values of cumulative emissions from 2015–2100 which keep temperature anomalies within 1.5 degrees of the pre-industrial baseline are 603 and 865 Gt C, respectively. For a 2 degree anomaly, these values are 782 and 1220 Gt C. Under all scenarios, the median temperature anomaly resulting from cumulative CO₂ emissions exceeds 1.5° C. The probabilities of exceeding 1.5 degree and 2 degree anomalies are provided in Table 2. As might be expected from Figure 1, delaying decarbonization results in substantially higher probabilities of exceeding these targets without taking into account non-CO₂ greenhouse gas emissions or other sources of CO₂ emissions, such as land-use changes.

We use a global sensitivity analysis [65, 66] to identify the drivers of temperature anomalies in 2100 resulting from 21st century CO₂ emissions. Global sensitivity analyses capture the effects of varying multiple parameters together, rather than focusing only on the impact of changing a single parameter (Fig. 3). TCRE, as the proportionality constant between emissions and warming, is the primary driver of temperature anomalies for the rest of the century, which explains the relatively similar levels of uncertainty in Figure 2. TCRE does not interact with our integrated assessment model variables, as it is an independent quantity which summarizes Earth-system processes. In the emissions model, 21st century cumulative emissions are largely driven by the rate of zero-carbon technology penetration, and so τ_4 , the half-saturation year of this technology, is the other variable of first-order importance. This is intuitive, as in this model, the dynamics of economic growth are mostly irrelevant with respect to emissions once the zero-carbon technology saturates. The speed of zero-carbon

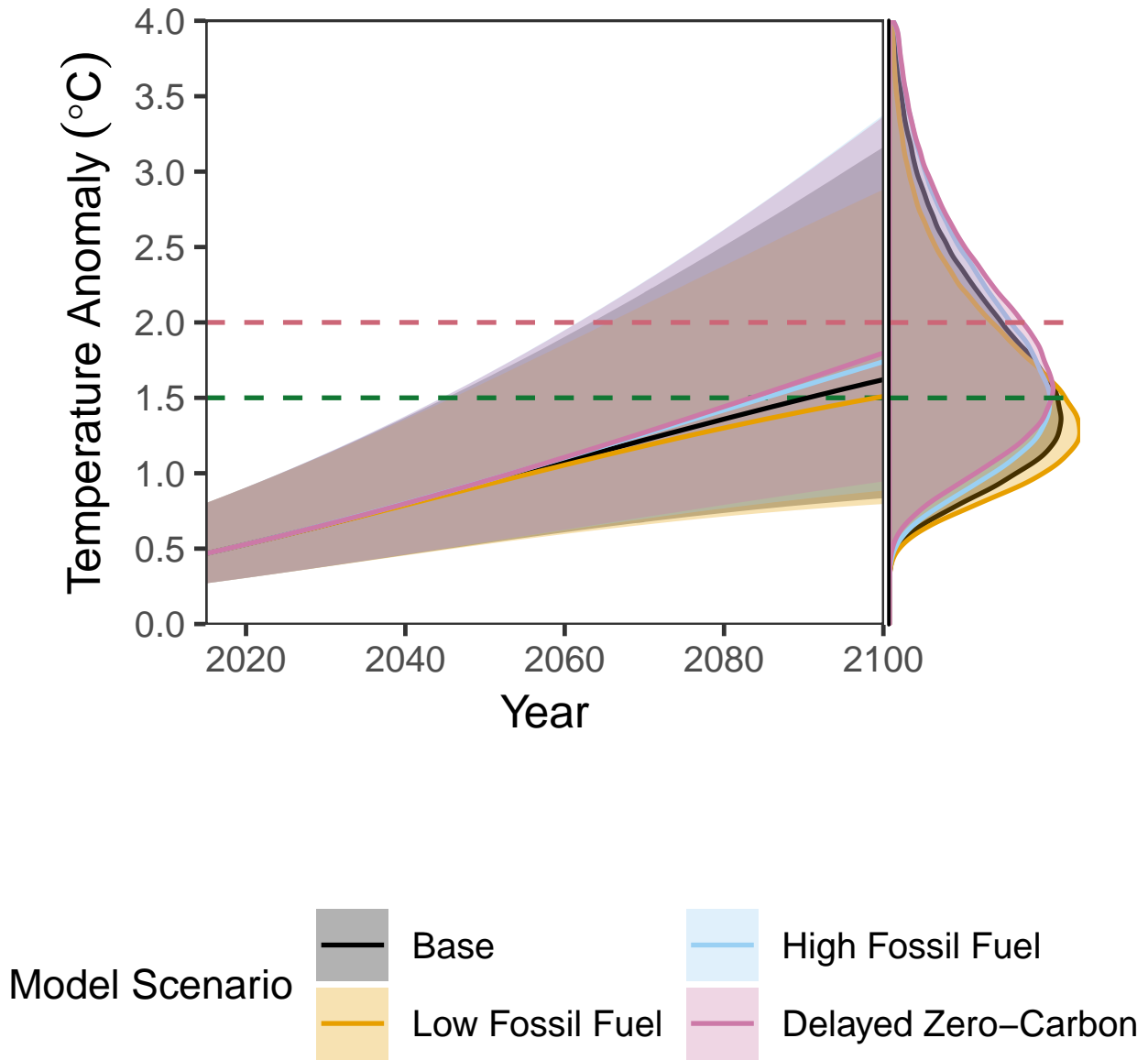


Figure 2: **Projections of temperature anomalies from CO₂ emissions** – Projections of global mean temperature anomalies (relative to the 1861-1880 mean) committed to by cumulative CO₂ emissions from 1870 through the plotted year. Projections are for four model scenarios: a) the base scenario; b) the low fossil fuel scenario; c) the high fossil fuel scenario; and d) the delayed zero-carbon scenario. The shaded regions are the 90% credible intervals. The marginal distribution of projected anomalies in 2100 is shown on the right. Projections include uncertainties in climate system responses using TCRE samples from a log-normal distribution fit to the 5-95% interval from [59]. The dashed lines correspond to the Paris temperature targets of 1.5° C (green) and 2° C (red) above pre-industrial temperatures.

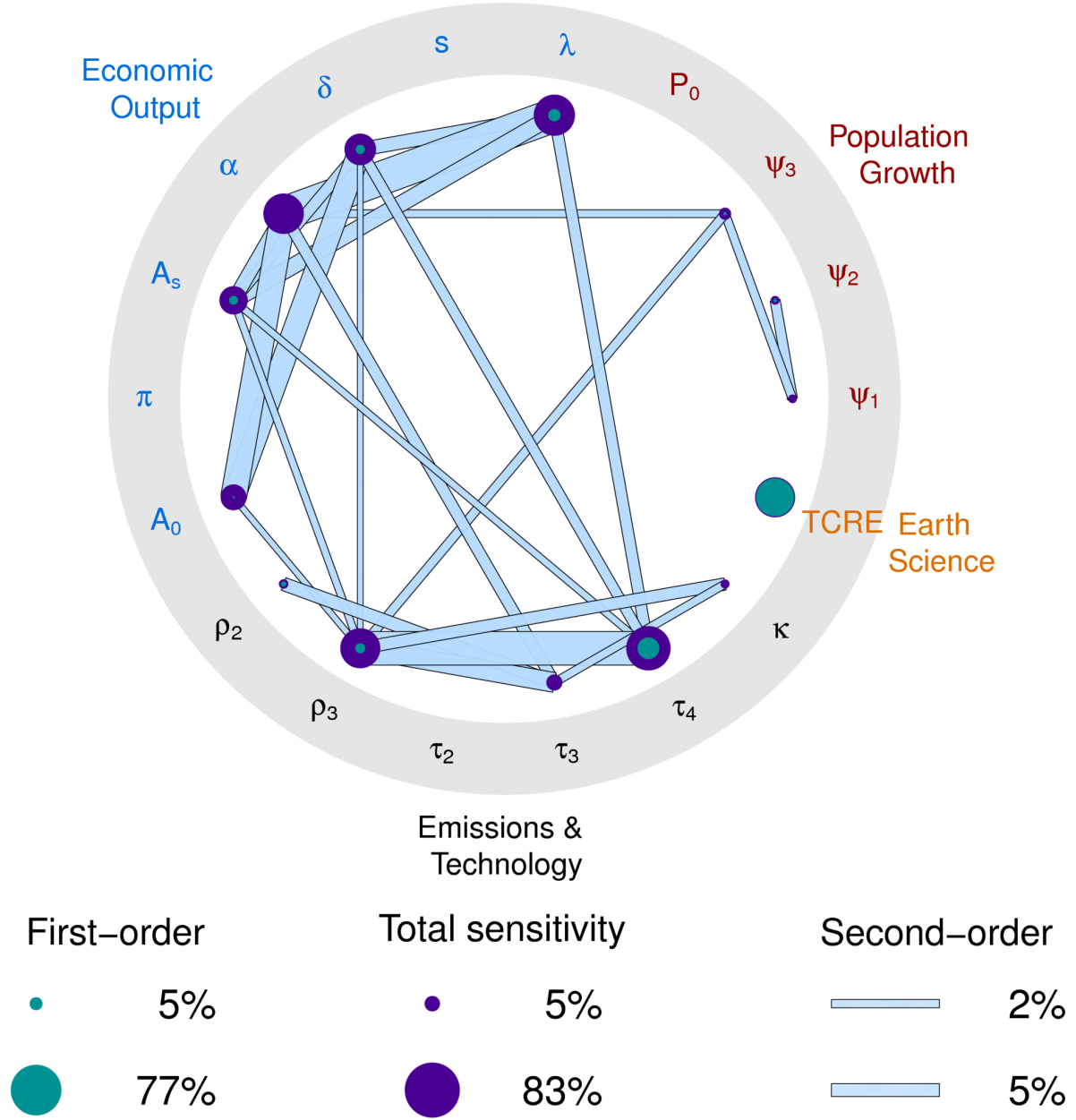


Figure 3: **Global sensitivity analysis for temperature anomalies** – Plot of Sobol' first-, second-, and total-order sensitivities for global mean temperature anomalies (relative to 1861–1880 average global mean temperature [61]) due to emissions from 2014 through 2100. The Sobol' analysis was based on an ensemble of model parameters jointly sampled from kernel density estimates around MCMC samples and TCRE samples from a log-normal distribution fit to the 5-95% interval from [59].

Table 2: **Probabilities of temperature anomalies committed by emissions through 2100 exceeding temperature targets** – Probabilities of temperature anomalies (relative to the 1861-1880 mean) committed to by cumulative CO₂ emissions *only* exceeding targets of 1.5° and 2° C. These exceedence probabilities are likely underestimates due to neglecting non-CO₂ greenhouse gas emissions [63]. Projections include uncertainties in climate system responses using TCRE samples from a log-normal distribution fit to the 5-95% interval from [59].

Model Scenario	P(Temp > 1.5° C)	P(Temp > 2° C)
Base	58%	30%
Low Fossil	51%	24%
High Fossil Fuel	64%	37%
Delayed Zero-Carbon	68%	39%

saturation also interacts with the total emissions associated with the reduced-emissions technology (ρ_3), which is the dominant technology prior to decarbonization.

Economic growth parameters can interact in important ways, as seen by the second-order sensitivities in Fig. 3. These sensitivities measure the impact of jointly varying parameters. For example, while the TFP growth rate α has no first-order effect on cumulative emissions, it is the third most important parameter with respect to total-order sensitivities, largely due to its interactions with the elasticity of production λ and the uncertain initial TFP A_0 . In the absence of decarbonization, this suggests that rapid changes in productivity and higher levels of elasticity with respect to capital are the main driver of emissions. This is due to the saturation of the labor pool, which is the result of the logistic model used for population and the assumption of a fixed labor participation rate, relative to continued economic growth. This economic growth is largely driven by TFP and capital (the rate of capital depreciation δ also has important total-order influence).

Population dynamics play only a small role in explaining the variance of cumulative emissions, though this could be due to our global aggregation of coupled population-economic dynamics. For example, population growth in Africa is a driver, in combination with other dynamics such as slow rates of regional agricultural productivity growth, of future states of the world in which policies aimed at mitigation do not reduce emissions as expected [67].

4 Discussion & Conclusions

Achieving temperature targets is a key objective of the internationally-ratified Paris agreement [68]. Thus far, the reduction of “business-as-usual” emissions response to this climate objective has been quite low in many countries [69]. It is hence important to understand the risks associated with business-as-usual dynamics, without policies aimed explicitly at mitigation. To this end, we derive probabilistic projections of emissions using a simple, calibrated integrated assessment model which assimilates century-scale data and expert assessments of economic growth. Despite the simplicity of the model structure, our projections agree well with historical growth and emissions trends.

We quantify the sensitivity of the emissions projections to the deeply uncertain quantity of remaining fossil fuel resources. This is largely due to the influence of this constraint on the required speed for decarbonizing the economy. In all scenarios, the emissions trajectories associated with RCPs 4.5 and 6.0 characterize two different “business-as-usual” modes, which depend on the speed of decarbonization. The plausibility of RCP 8.5 emissions (which is commonly thought of as a “business-as-usual” scenario [17]) depends on a large fossil fuel resource base, though it is a tail-risk scenario in all of our model scenarios. One essential note is that the forcings associated with RCP 8.5 might result from a lower level of emissions due to carbon-cycle uncertainty. This is important, as the impacts of climate change are the result of atmospheric concentrations of greenhouse gases, not simply from emissions. Thus, while RCP 8.5 may not be representative of a business-as-usual scenario (unlike RCPs 4.5 and 6.0), it has value for studies of climate change impacts as a high-risk, if low-probability, scenario.

We also show that the transient climate response to cumulative emissions and the rate of decarbonizing the economy have the strongest direct influence on resulting temperatures. Total factor productivity and capital input growth (and, correspondingly, the elasticity of production with respect to capital) are also important due to their total-order influence on economic growth. This suggests that, in the absence of rapid decarbonization, policies and market dynamics which result in strong increases in productivity and capital growth will result in a higher risk of worse climate outcomes.

Our posterior projections result in lower average GWP per-capita growth from 2010 to 2100 than previous work [27]. The previous study [27] considered per-capita GWP in both its model and expert assessment, while we model population and total GWP. This modeling difference is likely the source of the different projections, as our upper projections of per-capita GWP are similar when we assimilate data from 1820-2014 and 1950-2014. Per-capita growth that is stronger than our projections would result in higher emissions levels than we obtain.

As both the upper tail and the lower mode of our emissions projections are sensitive to the fossil fuel resource constraint, the risk of achieving temperature targets is strongly influenced by the size of this resource base. While there is a low probability under all of our considered scenarios that we can keep temperatures within 1.5 degrees C of 1880 temperatures, there is a large variation in our estimated probabilities of achieving a 2 degree C target. This probability can be narrowed by refining our estimate of TCRE, which can be constrained more readily by observations than equilibrium climate sensitivity [70], and by obtaining more reliable estimates of available fossil fuel resources, particularly those associated with unconventional oil and gas deposits.

Another crucial deep uncertainty is the rate of decarbonization. Fully decarbonizing the global economy will require a large amount of continued research and development and technology diffusion and global action across multiple sectors. This could occur naturally due to market dynamics or, though contrary to the business-as-usual assumption in this study, through coordinated climate mitigation policies. As hard as rapid decarbonization might be, it avoids the tension between economic growth and achieving climate targets.

Author Contributions

V.S., R.T., and K.K. designed the research. V.S. and K.K. conducted the research. V.S., Y.G., and K.K. analyzed the results. V.S., Y.G., R.T., and K.K. wrote the paper.

Acknowledgements

The authors thank Louise Miltich and Alexander Robinson for valuable inputs and contributions. We thank Arnulf Grübler, Jonathan Koomey, Robert Lempert, Michael Obersteiner, Brian O'Neill, Hugh Pitcher, Steve Smith, Rob Socolow, Dan Ricciuto, Mort Webster, Xi-aho Deng, Tony Wong, Jon Lamontagne, Emily Ho, and Billy Pizer for helpful discussions. This work was partially supported by the National Science Foundation (NSF) through the Network for Sustainable Climate Risk Management (SCRiM) under NSF cooperative agreement GEO-1240507 and the Penn State Center for Climate Risk Management. Any opinions, findings, and conclusions or recommendations expressed in this material are those of the authors and do not necessarily reflect the views of the NSF. All codes can be found at <http://www.github.com/vsrikrish/IAMUQ>.

References

- [1] Archer D, Ganopolski A (2005) A movable trigger: Fossil fuel CO₂ and the onset of the next glaciation. *Geochem. Geophys. Geosyst.* 6(5).
- [2] Bankes S (1993) Exploratory modeling for policy analysis. *Oper. Res.* 41(3):435–449.
- [3] Wigley TM, Raper SC (2001) Interpretation of high projections for global-mean warming. *Science* 293(5529):451–454.
- [4] Allen MR (2003) Climate forecasting: possible or probable? *Nature* 425(6955):242.
- [5] Barrie Pittock A, Jones RN, Mitchell CD (2001) Probabilities will help us plan for climate change. *Nature* 413(6853):249.
- [6] Kann A, Weyant JP (2000) Approaches for performing uncertainty analysis in large-scale energy/economic policy models. *Environ. Model. Assess.* 5(1):29–46.
- [7] Nordhaus WD, Yohe GW (1983) Future carbon dioxide emissions from fossil fuels in *Changing Climate: Report of the Carbon Dioxide Assessment Committee*, ed. National Research Council. (The National Academies Press, Washington, DC), pp. 87–153.
- [8] Schneider SH (2002) Can we estimate the likelihood of climatic changes at 2100? *Clim. Change* 52(4):441–451.
- [9] Webster M (2003) Communicating climate change uncertainty to policy-makers and the public. *Clim. Change* 61(1):1–8.

- [10] Mohr SH, Evans GM (2011) Long term forecasting of natural gas production. *Energy Policy* 39(9):5550–5560.
- [11] McGlade CE (2012) A review of the uncertainties in estimates of global oil resources. *Energy* 47(1):262–270.
- [12] McGlade C, Speirs J, Sorrell S (2013) Methods of estimating shale gas resources – comparison, evaluation and implications. *Energy* 59:116–125.
- [13] Mohr SH, Wang J, Ellem G, Ward J, Giurco D (2015) Projection of world fossil fuels by country. *Fuel* 141:120–135.
- [14] Ritchie J, Dowlatabadi H (2017) The 1000 GtC coal question: Are cases of vastly expanded future coal combustion still plausible? *Energy Econ.* 65:16–31.
- [15] Rogner HH (1997) An assessment of world hydrocarbon resources. *Annu. Rev. Energy Environ.* 22(1):217–262.
- [16] Quilcaille Y, et al. (2018) Uncertainty in projected climate change arising from uncertain fossil-fuel emission factors. *Environ. Res. Lett.* 13(4):044017.
- [17] Riahi K, et al. (2011) RCP 8.5—a scenario of comparatively high greenhouse gas emissions. *Clim. Change* 109(1):33.
- [18] Riahi K, et al. (2017) The shared socioeconomic pathways and their energy, land use, and greenhouse gas emissions implications: An overview. *Glob. Environ. Change* 42:153–168.
- [19] van Vuuren DP, de Vries B, Beusen A, Heuberger PSC (2008) Conditional probabilistic estimates of 21st century greenhouse gas emissions based on the storylines of the IPCC-SRES scenarios. *Glob. Environ. Change* 18(4):635–654.
- [20] Sokolov AP, et al. (2009) Probabilistic forecast for Twenty-First-Century climate based on uncertainties in emissions (without policy) and climate parameters. *J. Clim.* 22(19):5175–5204.
- [21] Raftery AE, Zimmer A, Frierson DMW, Startz R, Liu P (2017) Less than 2° C warming by 2100 unlikely. *Nat. Clim. Chang.* 7:637.
- [22] Pizer WA (1999) The optimal choice of climate change policy in the presence of uncertainty. *Res. Energy Econ.* 21(3):255–287.
- [23] Fuss S, et al. (2014) Betting on negative emissions. *Nat. Clim. Chang.* 4:850.
- [24] Smith P, et al. (2015) Biophysical and economic limits to negative CO₂ emissions. *Nat. Clim. Chang.* 6:42.
- [25] Vaughan NE, Gough C (2016) Expert assessment concludes negative emissions scenarios may not deliver. *Environ. Res. Lett.* 11(9):095003.

- [26] Hargreaves J, Annan J (2002) Assimilation of paleo-data in a simple Earth system model. *Clim. Dyn.* 19(5):371–381.
- [27] Christensen P, Gillingham K, Nordhaus W (2018) Uncertainty in forecasts of long-run economic growth. *Proc. Natl. Acad. Sci. U. S. A.* 115(21):5409–5414.
- [28] Bolt J, Inklaar R, de Jong H, van Zanden JL (2018) Maddison project database, version 2018 (<https://www.rug.nl/ggdc/historicaldevelopment/maddison/releases/maddison-project-database-2018>). Publication title: Rebasing 'Maddison': New income comparisons and the shape of long-run economic development, Maddison Project Working Paper 10.
- [29] Boden TA, Andres RJ, Marland G (2017) Global, regional, and national fossil-fuel CO₂ emissions (1751 - 2014) (v. 2017).
- [30] Nordhaus W, Sztorc P (2013) *DICE 2013R: Introduction and User's Manual*. Available at http://www.econ.yale.edu/~nordhaus/homepage/homepage/documents/DICE_Manual_100413r1.pdf, accessed 2019-5-10.
- [31] Nordhaus WD (2017) Revisiting the social cost of carbon. *Proc. Natl. Acad. Sci. U. S. A.* 114(7):1518–1523.
- [32] Cohen JE (1995) Population growth and earth's human carrying capacity. *Science* 269(5222):341–346.
- [33] Lutz W, Sanderson W, Scherbov S (2001) The end of world population growth. *Nature* 412(6846):543–545.
- [34] Starr C, Rudman R (1973) Parameters of technological growth. *Science* 182(4110):358–364.
- [35] Ausubel JH (1995) Technical progress and climatic change. *Energy Policy* 23(4):411–416.
- [36] Ruddiman WF (2003) The anthropogenic greenhouse era began thousands of years ago. *Clim. Change* 61(3):261–293.
- [37] Marchetti C (1977) Primary energy substitution models: On the interaction between energy and society. *Technol. Forecast. Soc. Change* 10(4):345–356.
- [38] Grübler A, Nakićenović N, Victor DG (1999) Dynamics of energy technologies and global change. *Energy Policy* 27(5):247–280.
- [39] McGlade C, Ekins P (2015) The geographical distribution of fossil fuels unused when limiting global warming to 2° C. *Nature* 517(7533):187–190.
- [40] Bruckner T, et al. (2014) Energy systems in *Climate Change 2014: Mitigation of Climate Change. Contribution of Working Group III to the Fifth Assessment Report of the Intergovernmental Panel on Climate Change*, eds. Edenhofer O, et al. (Cambridge University Press, Cambridge, United Kingdom).

- [41] Bayes T (1763) An essay towards solving a problem in the doctrine of chance. *Philosophical Transactions of the Royal Society of London* 53:370–418.
- [42] Brynjarsdóttir J, O’Hagan A (2014) Learning about physical parameters: the importance of model discrepancy. *Inverse Problems* 30:114007.
- [43] Storn R, Price K (1997) Differential evolution – a simple and efficient heuristic for global optimization over continuous spaces. *J. Global Optimiz.* 11(4):341–359.
- [44] Mullen K, Ardia D, Gil D, Windover D, Cline J (2011) DEoptim: An R package for global optimization by differential evolution. *Journal of Statistical Software, Articles* 40(6):1–26.
- [45] Metropolis N, Rosenbluth AW, Rosenbluth MN, Teller AH, Teller E (1953) Equation of state calculations by fast computing machines. *J. Chem. Phys.* 21(6):1087–1092.
- [46] Hastings WK (1970) Monte Carlo sampling methods using Markov chains and their applications. *Biometrika* 57(1):97–109.
- [47] Gelman A, Rubin DB (1992) Inference from iterative simulation using multiple simulations. *Stat. Sci.* 7(4):457–511.
- [48] Tippet MK, DelSole T, Barnston AG (2014) Reliability of Regression-Corrected climate forecasts. *J. Clim.* 27(9):3393–3404.
- [49] IIASA (2009) RCP database (<https://tntcat.iiasa.ac.at/RcpDb>). Accessed: 2019-5-22.
- [50] Loftus PJ, Cohen AM, Long JCS, Jenkins JD (2015) A critical review of global decarbonization scenarios: What do they tell us about feasibility? *WIREs Clim Change* 6(1):93–112.
- [51] van Vuuren DP, et al. (2011) The representative concentration pathways: an overview. *Clim. Change* 109(1):5.
- [52] O’Neill BC, et al. (2014) A new scenario framework for climate change research: the concept of shared socioeconomic pathways. *Clim. Change* 122(3):387–400.
- [53] O’Neill BC, et al. (2017) The roads ahead: Narratives for shared socioeconomic pathways describing world futures in the 21st century. *Glob. Environ. Change* 42:169–180.
- [54] Friedlingstein P, et al. (2014) Uncertainties in CMIP5 climate projections due to carbon cycle feedbacks. *J. Clim.* 27(2):511–526.
- [55] Mastrandrea MD, et al. (2011) The IPCC AR5 guidance note on consistent treatment of uncertainties: a common approach across the working groups. *Clim. Change* 108(4):675.
- [56] Kriegler E, et al. (2017) Fossil-fueled development (SSP5): An energy and resource intensive scenario for the 21st century. *Glob. Environ. Change* 42:297–315.

- [57] Ritchie J, Dowlatabadi H (2017) Why do climate change scenarios return to coal? *Energy* 140:1276–1291.
- [58] Matthews HD, Gillett NP, Stott PA, Zickfeld K (2009) The proportionality of global warming to cumulative carbon emissions. *Nature* 459(7248):829–832.
- [59] Gillett NP, Arora VK, Matthews D, Allen MR (2013) Constraining the ratio of global warming to cumulative CO₂ emissions using CMIP5 simulations. *J. Clim.* 26(18):6844–6858.
- [60] MacDougall AH, Friedlingstein P (2015) The origin and limits of the near proportionality between climate warming and cumulative CO₂ emissions. *J. Clim.* 28(10):4217–4230.
- [61] Morice CP, Kennedy JJ, Rayner NA, Jones PD (2012) Quantifying uncertainties in global and regional temperature change using an ensemble of observational estimates: The HadCRUT4 data set: THE HADCRUT4 DATASET. *J. Geophys. Res.* 117(D8).
- [62] Collins M, et al. (2013) Long-term climate change: Projections, commitments and irreversibility in *Climate Change 2013: The Physical Science Basis. Contribution of Working Group I to the Fifth Assessment Report of the Intergovernmental Panel on Climate Change*, eds. Stocker TF, et al. (Cambridge University Press, Cambridge, UK and New York, NY).
- [63] Tokarska KB, Gillett NP, Arora VK, Lee WG, Zickfeld K (2018) The influence of non-CO₂ forcings on cumulative carbon emissions budgets. *Environ. Res. Lett.* 13(3):034039.
- [64] Gernaat DEHJ, et al. (2015) Understanding the contribution of non-carbon dioxide gases in deep mitigation scenarios. *Glob. Environ. Change* 33:142–153.
- [65] Saltelli A (2002) Making best use of model evaluations to compute sensitivity indices. *Comput. Phys. Commun.* 145(2):280–297.
- [66] Sobol’ IM (1993) Sensitivity estimates for nonlinear mathematical models. *Mathematical Modeling and Computational Experiment* 1(4):407–414.
- [67] Lamontagne JR, et al. (2018) Large ensemble analytic framework for Consequence-Driven discovery of climate change scenarios. *Earth’s Future* 6(3):488–504.
- [68] Schleussner CF, et al. (2016) Science and policy characteristics of the paris agreement temperature goal. *Nat. Clim. Chang.* 6(9):827.
- [69] UNEP (2018) Emissions gap report 2018, (United Nations Environmental Programme, Nairobi), Technical report.
- [70] Knutti R, Rugenstein MAA, Hegerl GC (2017) Beyond equilibrium climate sensitivity. *Nat. Geosci.* 10:727.

Supplemental Information

1 Derivation of VAR(1) Likelihood Function

Let $x_t = z_t - M(\theta)_t$, where z_t is the observation at time t and $M(\theta)_t$ is the model output at time t . We assume a VAR(1) process for the model residuals, and that there are iid observation errors. The model for a VAR(1) process with observation errors is:

$$\begin{aligned}x_t &= Ax_{t-1} + w_t \\ y_t &= x_t + \varepsilon_t,\end{aligned}$$

where $w_t \sim N(0, W)$ and $\varepsilon_t \sim N(0, D)$, with D the diagonal matrix of observation errors. We assume that $\text{Cov}(\varepsilon_t, \varepsilon_s) = 0$ for $t \neq s$, and the same for $\text{Cov}(w_t, w_s)$. Further, the process (x_t) is weakly stationary with $E(x_t) = 0$.

The covariance of y_t is

$$\begin{aligned}\Sigma_y &= \text{Cov}(y_t) \\ &= E[(x_t + \varepsilon_t)(x_t + \varepsilon_t)'] \\ &= E(x_t x_t') + E(\varepsilon_t \varepsilon_t') \\ &= \Sigma_x + D\end{aligned}$$

And

$$\begin{aligned}\Sigma_x &= \text{Cov}(x_t) \\ &= E[(Ax_{t-1} + w_t)(Ax_{t-1} + w_t)'] \\ &= AE(x_{t-1} x_{t-1}')A' + E(w_t w_t') \\ &= A\Sigma_x A' + W\end{aligned}$$

Then

$$\begin{aligned}\text{vec}(\Sigma_x) &= (A \otimes A)\text{vec}(\Sigma_x) + \text{vec}(W) \\ \text{vec}(\Sigma_x) &= (I - A \otimes A)^{-1}\text{vec}(W).\end{aligned}$$

The lag- h covariance is

$$\begin{aligned}\text{Cov}(y_t, y_{t-h}) &= A^h \text{Cov}(x_{t-1}, x_{t-h}) \\ &= A^h \Sigma_x.\end{aligned}$$

Then $(y_t) \sim N(0, \Sigma)$, where

$$\Sigma = \begin{pmatrix} \Sigma_x + D & (A\Sigma_x)' & \dots & (A^{n-1}\Sigma_x)' \\ A\Sigma_x & \Sigma_x + D & \dots & (A^{n-2}\Sigma_x)' \\ \vdots & \vdots & \ddots & \vdots \\ A^{n-1}\Sigma_x & A^{n-2}\Sigma_x & \dots & \Sigma_x + D \end{pmatrix}.$$

2 Prior Distributions and Sensitivities

2.1 Default Priors

Tables S1 and S2 list the prior distributions for the model. Prior distributions are specified by their family (*e.g.* normal or uniform) and a lower and upper bound. Normal-family distributions (including normal and log-normal distributions) are specified using their 5% and 95% central confidence limits, while uniform distributions are specified using their lower and upper bounds.

Table S1: Prior distributions used in calibration for the model parameters. Lower and upper bounds are absolute bounds for uniform distributions and central 95% confidence limits for normal and log-normal distributions.

Parameter	Description	Units	Prior	Lower Bound	Upper Bound	Reference
ψ_1	population growth rate	1/year	normal	0.0001	0.15	this study
ψ_2	half-saturation constant	1000\$/ (year capita)	uniform	0	50	this study
ψ_3	population carrying capacity	billions	normal	6.9	14.4	[1] ^a
P_0	population in 1700	billions	normal	0.3	0.9	[2] ^b
λ	elasticity of production with respect to labor	dimensionless	normal	0.6	0.8	[3]
s	savings rate	dimensionless	normal	0.22	0.26	this study ^c
δ	capital depreciation rate	1/year	uniform	0.01	0.14	[4, 5]
α	rate of technological progress	1/year	normal	0.0007	0.0212	this study
A_s	saturation level of total factor productivity	dimensionless	uniform	5.3	16.11	[4] ^d
π	labor participation rate	dimensionless	normal	0.62	0.66	this study ^e
A_0	total factor productivity in 1700	dimensionless	uniform	0	3	this study ^f
ρ_2	carbon intensity of technology 2	kg carbon/2011US\$	normal	0	0.75	this study
ρ_3	carbon intensity of technology 3	kg carbon/2011US\$	normal	0	0.75	this study
τ_2	half-saturation year of technology 2	year	uniform	1700	2100	this study
τ_3	half-saturation year of technology 3	year	uniform	1700	2100	this study
τ_4	half-saturation year of technology 4	year	uniform	2020	2500	this study
κ	rate of technological penetration	1/year	uniform	0.005	0.2	[6]

^a The lower bound is the peak population in the 2.5% scenario; the upper bound the 2100 population in the 97.5% scenario.

^b The lower bound is the minimum of the four alternative estimates of [2, Table B-1] minus the standard deviation; the upper bound is the maximum plus the standard deviation.

^c The global average gross savings rate between 1977 and 2017 is 24% with a standard deviation of 1.1% [7]. The range given here is consistent with that distribution.

^d We use the ratio of the 2005 level to the long-term saturation level with a uniform probability density function of $\pm 50\%$.

^e The global average labor force participation rate between 1990 and 2018 is 64% with a standard deviation of 1.4% [8]. The range given here is consistent with that distribution.

^f The best guess is obtained using $A_0 = Q_0 \lambda / (1 + \lambda) (\delta / s)^{\lambda / (1 + \lambda)} (\pi P_0)^{\lambda^2 / (1 + \lambda)}$.

Table S2: Prior distributions used in calibration for the statistical parameters.

Parameter	Description	Units	Prior	Lower Bound	Upper Bound	Reference
a_{ii}	diagonal entries of VAR coefficient matrix A	dimensionless	normal	0	1	this study
$a_{ij}, i \neq j$	off-diagonal entries of VAR coefficient matrix A	dimensionless	normal	-1	1	this study
σ_1	log-scale population innovation variance	(log-billions) ²	log-normal	0	∞	this study ^a
σ_2	log-scale GWP innovation variance	(log-trillions 2011USD\$) ²	log-normal	0	∞	this study ^a
σ_3	log-scale emissions innovation variance	(log-GtC/yr) ²	log-normal	0	∞	this study ^a
ε_1	log-scale population observation error variance	(log-billions) ²	log-normal	0	∞	this study ^a
ε_2	log-scale GWP observation error variance	(log-trillions 2011USD\$) ²	log-normal	0	∞	this study ^a
ε_3	log-scale emissions observation error variance	(log-GtC/yr) ²	log-normal	0	∞	this study ^a

^a Log-normal distributions have log-scale means of -1 and log-scale standard deviations of 1.

2.2 Sensitivity to Priors

Table S3 specifies alternate priors for particular parameters to detect the sensitivity of projections to the choice of priors. These parameters were selected because they were either identified as important by the sensitivity analysis (Figure 2) or they were not updated by the Bayesian inversion (Figure S2). The alternate prior specifications were selected to include unbounded prior ranges (when the prior was previously uniform) or fatter tails (when the prior was previously normal). Other priors are kept the same from the base scenario.

Figure S1 shows the projections resulting from calibrating the model with these prior distributions. In general, the projections are identical, and the qualitative features of the marginal distribution in 2100 are preserved.

Table S3: Prior distributions used in calibration for the model parameters. Lower and upper bounds are absolute bounds for uniform distributions and central 95% confidence limits for normal and log-normal distributions.

Parameter	Description	Units	Prior	Lower Bound	Upper Bound	Reference
λ	elasticity of production with respect to labor	dimensionless	log-normal	0.6	0.8	
s	savings rate	dimensionless	log-normal	0.22	0.26	
A_s	saturation level of total factor productivity	dimensionless	normal	5.3	16.11	
π	labor participation rate	dimensionless	log-normal	0.62	0.66	

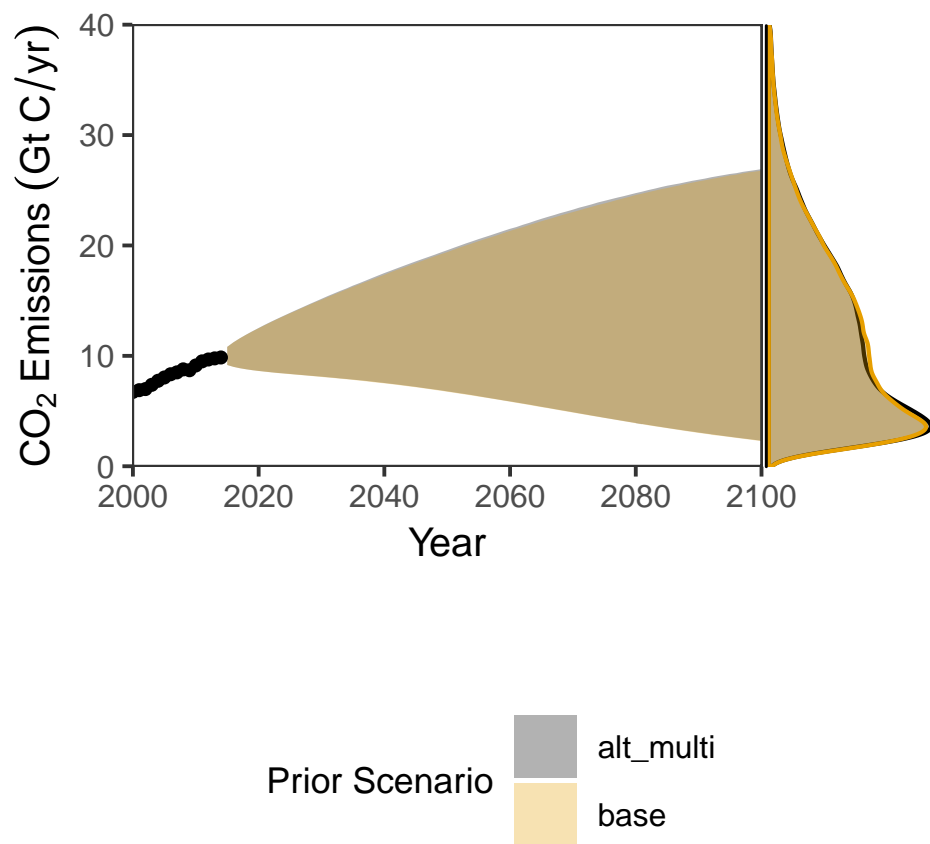


Figure S1: **Sensitivity of carbon dioxide emissions projections to prior distributions** – Projections are for the default priors (Table S1 and Table S2) and an alternate set of priors (Table S3). The shaded regions are the 90% credible intervals. Black dots are observations. The marginal distribution of projected business-as-usual CO₂ emissions in 2100 is shown on the right.

3 Supplemental Figures

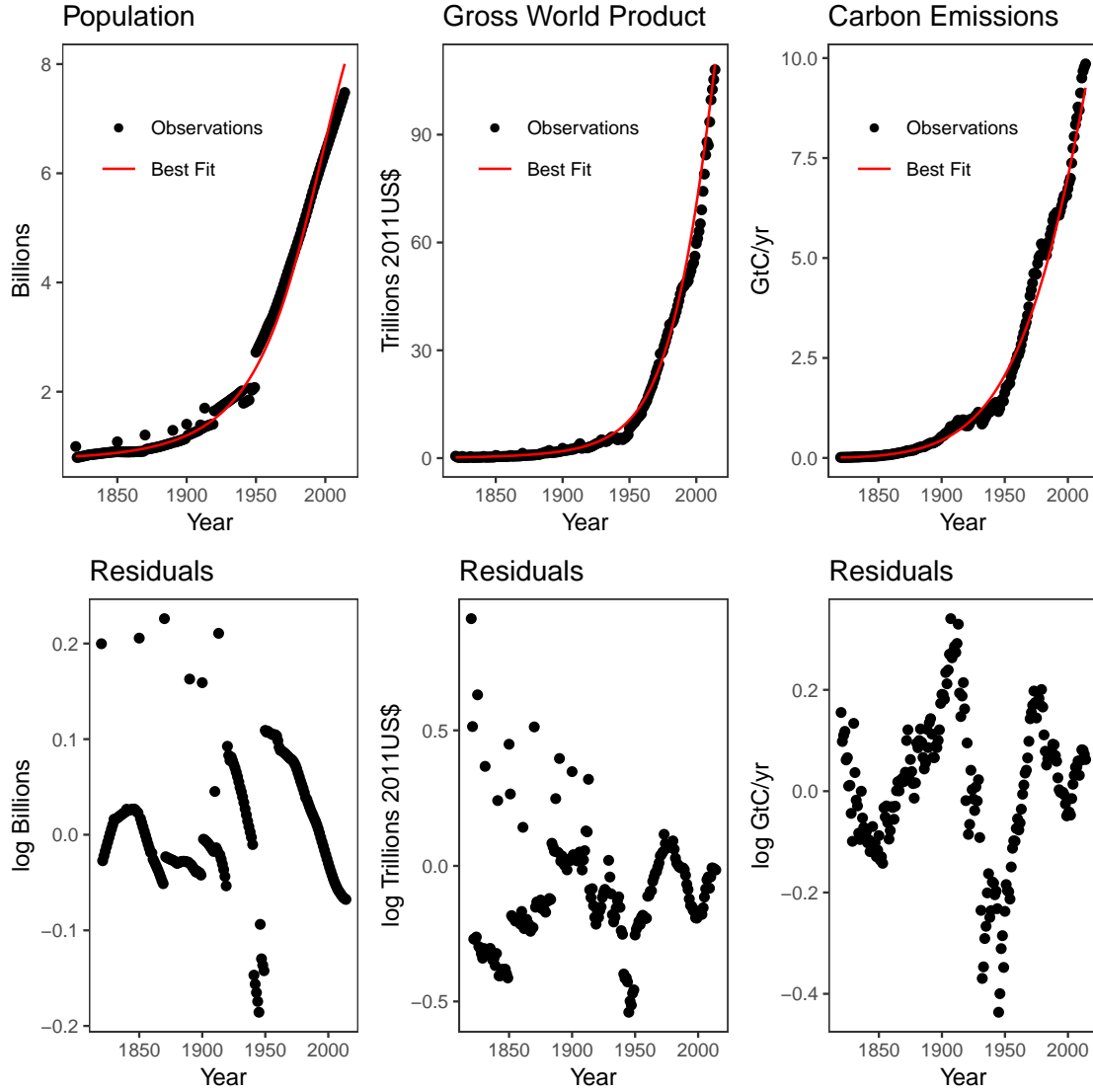


Figure S2: **Model fit and residuals under an independent-and-identically-distributed residual assumption** – Model fit and residuals of the log-model fit for MAP estimate of parameter values when assuming that the residuals are independent and identically distributed. The lag-1 autocorrelations are 0.60 for population residuals, 0.49 for GWP residuals, and 0.94 for emissions residuals. The lag-0 cross-correlations range from 0.13 to 0.58, and the lag-1 cross-correlations range from 0.06 to 0.54.

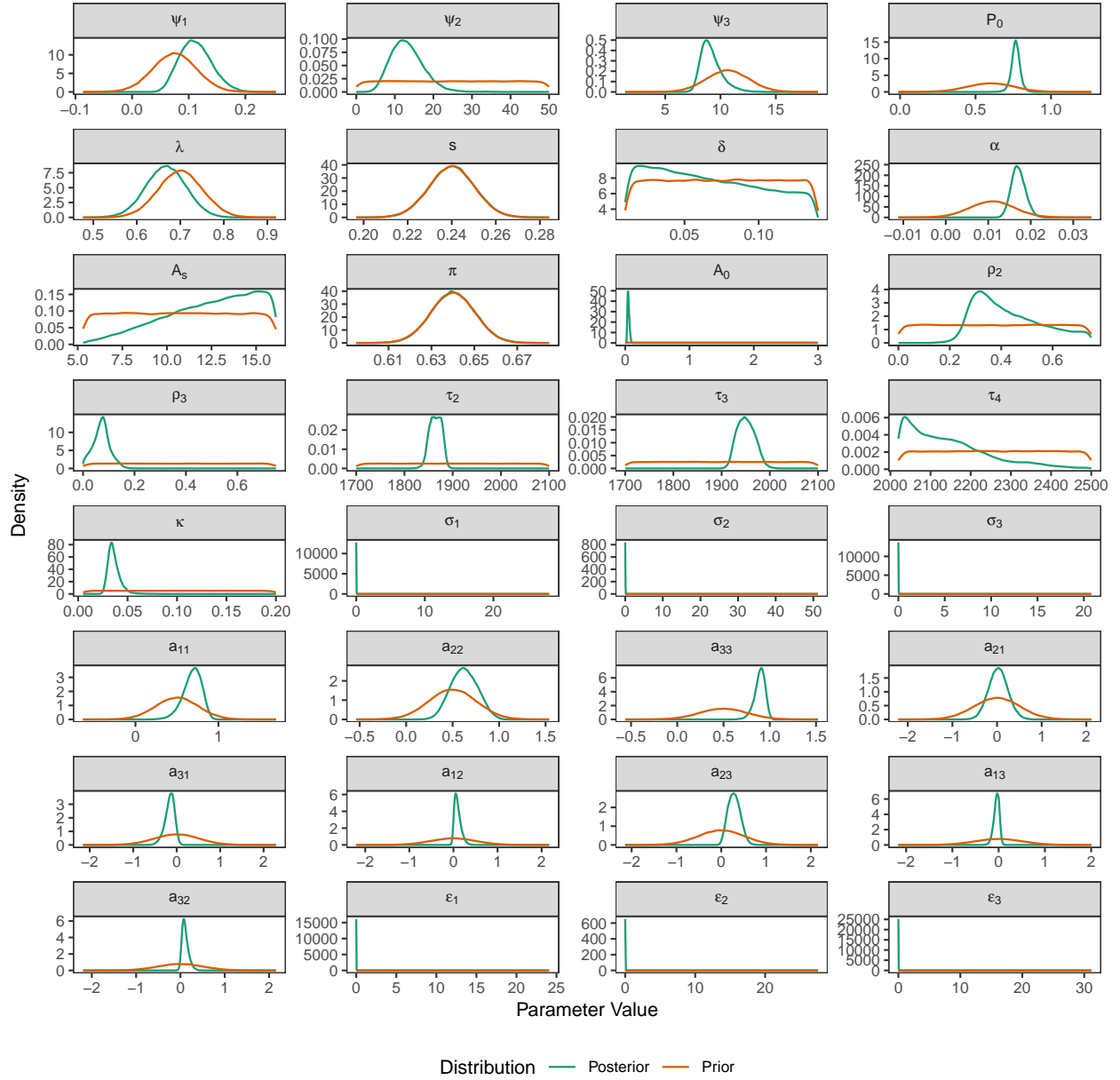


Figure S3: **Prior and posterior distributions for model parameters** – Prior and posterior distributions for the model parameters under the “base” fossil fuel resource scenario. Prior distributions are in orange; posterior distributions are in red.

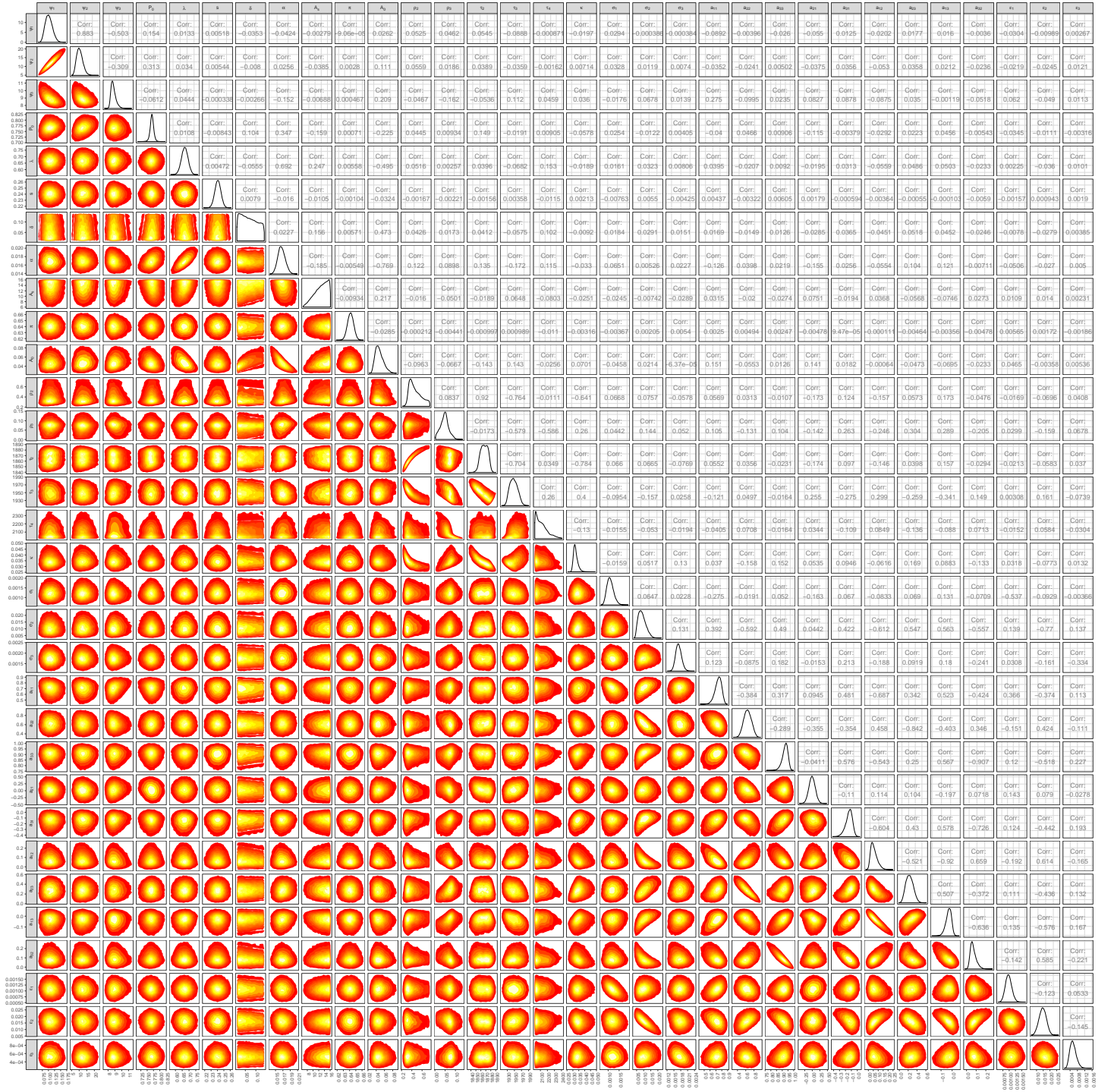


Figure S4: **Pairs plots for the base model calibration** – Pairs plots for the model calibration under the “base” fossil fuel resource constraint. In the lower triangle are heat maps showing the pairwise posterior densities. The main diagonal consists of marginal posterior density plots, and the upper triangle shows the correlations between the corresponding variables.

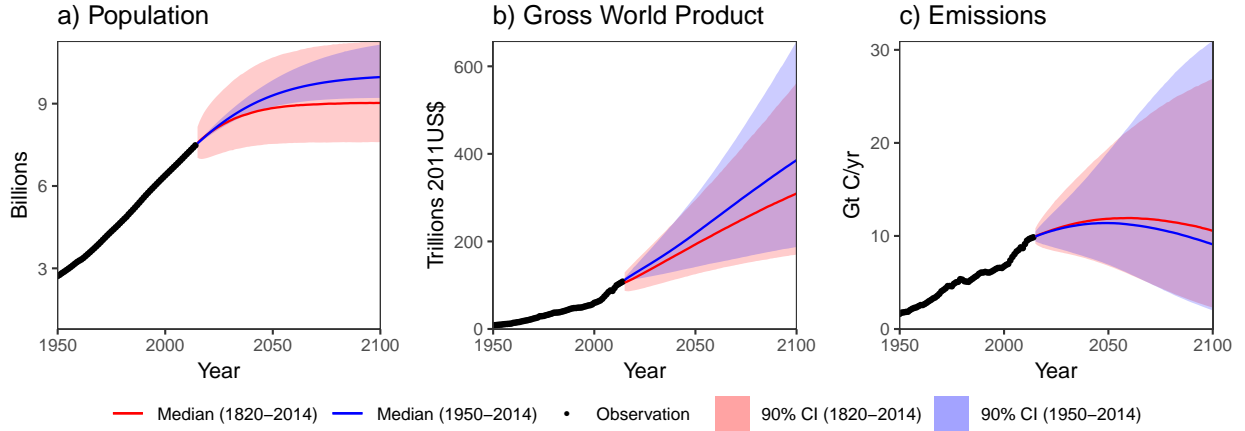


Figure S5: **Comparison of hindcasts and projections for different data lengths** – Comparison of hindcasts and projections from 1900-2100 for the model (with base assumptions about fossil fuel resources and zero-carbon half-saturation year prior densities) calibrated with data from 1820-2014 (red) and 1950-2014 (blue) for: a) global population, b) gross world product, c) CO₂ emissions. The ribbons are the 90% credible intervals, and the lines are the posterior medians.

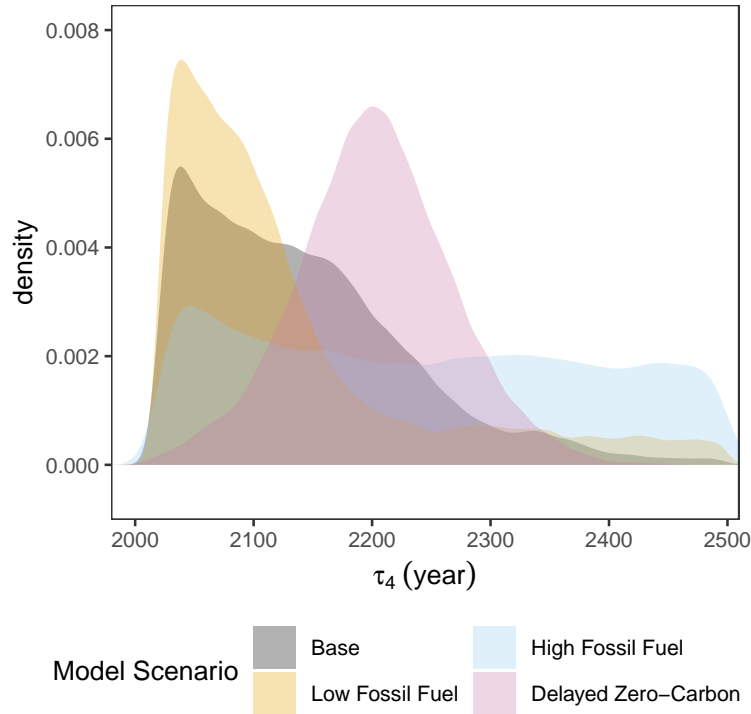


Figure S6: **Marginal distribution of zero-carbon half-saturation year by scenario** – Marginal distribution of τ_4 , the half-saturation year of zero-carbon technology, by model scenario.

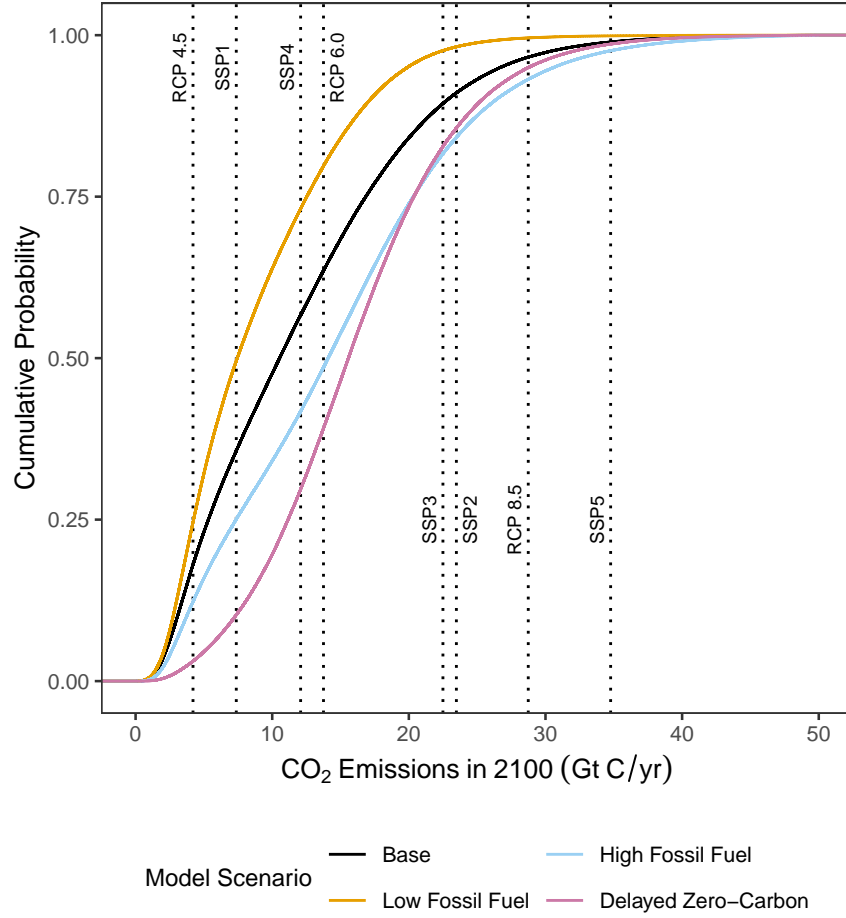


Figure S7: **Cumulative distribution functions of emissions projections in 2100 by model scenario** – Cumulative distribution functions of CO₂ emissions projections in 2100 for each model scenario. Representative Concentration Pathway (RCP). and Shared Socioeconomic Pathway (SSP) emissions values in 2100 are displayed as dotted lines.

References

- [1] Lutz W, Sanderson W, Scherbov S (1997) Doubling of world population unlikely. *Nature* 387(6635):803–805.
- [2] Maddison A (2003) *The World Economy*. (OECD), p. 274.
- [3] Romer D (2012) *Advanced Macroeconomics*. (McGraw-Hill/Irwin, New York), Fourth edition.
- [4] Nordhaus WD (1994) *Managing the global commons : the economics of climate change*. (MIT Press, Cambridge, Mass.).
- [5] Nadiri MI, Prucha IR (1996) Estimation of the depreciation rate of physical and r&d capital in the U.S. total manufacturing sector. *Econ. Inq.* 34(1):43–56.
- [6] Grubler A (1991) Diffusion: Long-term patterns and discontinuities. *Technol. Forecast. Soc. Change* 39(1):159–180.
- [7] World Bank (2018) Gross savings (% of GDP) (<https://data.worldbank.org/indicator/ny.gns.ictr.zs?end=2017&start=1960&view=chart>). Accessed: 2019-5-15.

- [8] World Bank (2019) Labor force participation rate, total (% of total population ages 15+) (<https://data.worldbank.org/indicator/sl.tlf.cact.zs>). Accessed: 2019-5-15.